

# Waste-to-Energy-Coupled AI Data Centers: Cooling Efficiency and Grid Resilience

Qi He  
Google LLC  
USA

Chunyu Qu  
Dun & Bradstreet Inc  
USA

## Abstract

AI data-center expansion is increasingly constrained by the coupled availability of deliverable electricity and heat-rejection (cooling) capacity. We propose and evaluate an integrated Waste-to-Energy-AI Data Center configuration that treats cooling as a first-class energy service rather than an unavoidable electricity burden. The coupled system is modeled as an input-output “black box” with transparent boundaries and a standalone benchmark in which mechanical chilling is powered by grid electricity. The central mechanism is energy-grade matching: low-grade WtE thermal output drives absorption cooling to deliver chilled service, thereby displacing baseline cooling electricity. We show that thermoeconomic superiority is governed by three first-order determinants, (i) cooling coverage of IT heat load, (ii) parasitic electricity for transport and auxiliaries, and (iii) distance-driven delivery decay, yielding a break-even corridor beyond which net benefits vanish. Comparative statics characterize sensitivity to IT utilization, feedstock quality (waste LHV and throughput), climate parameterization, and corridor distance. We translate these accounting gains into decision language through a computable prototype for Levelized Cost of Computing (LCOC) and an ESG valuation channel grounded in measurable mechanisms, without re-deriving full lifecycle inventories. The framework provides siting-ready feasibility conditions for WtE-AIDC coupling in urban AI corridors under grid stress.

**Keywords** - *AI data centers, Absorption cooling, Waste-to-energy (WtE), Power Usage Effectiveness (PUE), Thermally driven cooling, Energy resilience, Energy-service valuation*

## Introduction

AI data-center expansion is increasingly constrained not by model architectures but by the joint availability of deliverable energy services, reliable electricity and heat rejection at scale. Recent assessments emphasize that data centers (DCs) have already become a material electricity load and that AI-driven growth could sharply increase demand over the next decade [1], [2]. What binds, however, is often local and physical rather than global and abstract: grid-constrained interconnections, long equipment lead times, and community limits on thermal and water footprints. What is scarce is not “compute” in the abstract, but the capacity to deploy compute within a feasible electricity–cooling envelope.

Cooling is central to that envelope because it governs both operating cost and feasible power density. Conventional mechanical cooling uses high-grade electricity to move low-grade heat to ambient; even with containment, economizers, and advanced controls, it remains anchored to compressor and fan work that scales with thermal load. This motivates the ongoing transition toward liquid-assisted architectures. Yet the most widely deployed forms of liquid cooling primarily improve heat transfer near the chip or rack, while the facility still depends, partially or fully, on electricity-driven chillers, cooling towers, dry coolers, or hybrid mechanical systems for ultimate heat rejection [3]. The practical consequence is that cooling remains a first-order driver of marginal electricity demand and siting feasibility, even as the industry improves thermal density.

This paper proposes a complementary pathway: treat cooling as an energy service that can be supplied through grade matching, using low-grade thermal energy to produce delivered cooling via thermally driven cycles, thereby displacing compressor electricity. The grade-matching opportunity is particularly salient in urban regions where two infrastructures often co-locate yet remain “accounting-separate”: municipal solid-waste treatment and compute campuses. Municipal solid waste (MSW) contains recoverable chemical energy; when landfilled, its organic fraction generates methane under anaerobic decomposition. Because methane is a short-lived but high-impact greenhouse gas, the near-term climate cost of uncontrolled releases is especially salient in both science and policy [4], [5]. This provides a natural systems context for reconsidering how urban waste streams can be converted into useful services, especially in grid-stressed AI corridors.

Qu and He (2025) established a clean narrative entry point for waste-sector interventions motivated by AI-era grid resilience [6]. It clarified why methane-dominant baselines matter for near-term climate risk and why waste-linked energy recovery should be evaluated as a targeted control volume for buffering critical loads rather than as a generic substitute for renewables. The present paper is intentionally narrower and more decision-direct: we focus on the coupling mechanism that converts WtE thermal outputs into a delivered cooling service for AI DCs, and we quantify when that coupling is thermoeconomically superior under realistic spatial and parasitic constraints.

A common barrier to taking waste-to-energy (WtE) seriously in the AI-infrastructure context is the perception that WtE is intrinsically “dirty.” That perception is historically understandable but technically incomplete. Modern plants operate under stringent pollutant control regimes, and leading jurisdictions encode these expectations into enforceable standards. The European Union’s BAT Conclusions for waste incineration formalize best-available techniques and associated emissions performance levels [7]. In the United States, large municipal waste combustors are regulated under the Clean Air Act with detailed performance standards and compliance requirements [8]. China’s national standards have also evolved

and are publicly documented, reflecting a tightening emissions-control regime for MSW incineration [9]. Large-sample empirical evidence from China further treats pollutant control and resource recovery as measurable performance levers rather than fixed constraints [10]. We emphasize these points only to set the legitimacy boundary condition: this paper does not re-litigate whether WtE should exist; it evaluates whether, conditional on a modern regulated plant, there is an economically meaningful gain from coupling WtE outputs to AI cooling demand.

## Related Work and Positioning

A large engineering and operations literature focuses on reducing cooling energy through airflow management, economization, controls, and alternative cooling architectures. In practice, decision-making is often mediated through facility-level KPIs, especially Power Usage Effectiveness (PUE), because PUE provides a standardized accounting ratio connecting IT load to total facility energy use [2], [11]. PUE is useful precisely because it is an accounting object: it translates heterogeneous engineering choices into a comparable energy burden per unit IT power. However, PUE is often interpreted narrowly as an efficiency score rather than as an equilibrium outcome of energy-service substitution, i.e., what fraction of “support energy” can be displaced by alternative service pathways that do not consume high-grade electricity.

The post-2020 acceleration of liquid cooling is driven by thermal-density constraints: cold plates and immersion improve near-chip heat transfer and reduce reliance on high-volume air handling. Yet recent reviews emphasize that many liquid-cooled deployments still require electricity-driven systems for ultimate heat rejection (chillers, dry coolers, cooling towers, or hybrids), meaning the marginal cooling service is still largely purchased as electricity [3]. It reflects the deeper fact that most facilities remain electric-to-cooling at the plant boundary.

A parallel literature examines waste heat recovery from DCs and other industrial loads for district heating and integrated energy systems. Post-2020 reviews synthesize pathways (air exhaust, warm-water loops, refrigerant-based systems), utilization modes (space heating, district heat, industrial/agricultural uses), and enabling conditions (temperature level, temporal matching, and infrastructure constraints) [12]. Recent “DC integrated energy system” (DC-IES) frameworks explicitly argue that the DC should be modeled as a node in a multi-energy network where heat, power, and storage co-optimize [13]. Within this space, absorption systems are a canonical technology for converting thermal energy into cooling, but most analyses either (i) remain equipment-centric (cycle design, working pairs, heat exchangers), or (ii) abstract away the spatial delivery constraint, the fact that cooling (or the thermal input that produces it) must be delivered through real corridors with losses and pumping work. Very recent studies do begin to formalize thermally driven refrigeration with storage and advanced integration, but they typically still assume an available heat source and do not generalize to a siting-ready break-even frontier for urban WtE–AIDC corridors [14].

The WtE literature spans lifecycle comparisons (landfill vs. incineration with energy recovery), plant performance heterogeneity, and regulated emissions regimes. For this paper, the key point is not to re-argue global optimality, but to clarify the relevant boundary: conditional on a modern regulated WtE plant, there exists a residual thermal stream whose utilization can be economically meaningful if it displaces high-grade electricity otherwise used for cooling. The existence of stringent regulatory frameworks is well documented across major jurisdictions [7]–[9], and new empirical work at scale underscores how pollutant control and resource recovery can materially shift environmental and economic performance [10].

Because grade matching is fundamentally about “energy quality,” we adopt a thermoeconomic lens that distinguishes high-grade electricity from low-grade heat. Thermoeconomics and exergy-based methods provide a rigorous framework for assigning economic meaning to energy transformations when multiple streams of different quality coexist [15]. Modern exergy/exergoeconomic studies continue to operationalize these ideas for low-grade heat recovery and thermally driven cycles, offering practical balance equations and cost-allocation logic that align with engineering conservation constraints while remaining decision-relevant [16]. In our setting, exergy is not a decorative thermodynamics addition; it is the quality-adjusted bookkeeping needed to compare a baseline that purchases electricity for cooling against a coupled system that supplies cooling via thermal recovery.

### Gap and contribution

Despite rapid progress in each silo, existing work lacks a unified, computable framework that brings together: (i) delivered cooling service (not just “available heat”), (ii) distance-driven decay and parasitics (thermal losses and pumping work as first-order constraints), and (iii) a direct interface to project metrics such as break-even corridors and a prototype Levelized Cost of Computing (LCOC). This gap matters because real projects often fail not because absorption chillers cannot be engineered, but because delivered service net of losses is insufficient or because spatial decay eliminates benefit beyond a short corridor.

Figure 1 therefore presents the coupled WtE–AIDC system as an input–output “black box” with explicit accounting for electricity, thermal energy, and cooling service alongside a transparent standalone baseline. Figure 2 details the energy-cascade logic, electricity as a high-grade stream and thermal recovery as a low-grade stream that can be upgraded into cooling service, and makes the “avoided electricity” pathway physically interpretable. These figures also clarify our modeling boundary: evaluate the coupling at the energy-service accounting level, because project viability is first-order determined by coverage, parasitics, and spatial decay; equipment-level design is second-order and can be optimized conditional on these boundary constraints.

Our contribution is thus thermoeconomic and systems-strategic rather than equipment-specific. We (i) formalize minimal conservation-consistent boundaries for electricity/heat/cooling accounting in the integrated WtE–AIDC topology (Section 2) and link operational efficiency metrics such as PUE to an economic interpretation via energy-service substitution (Section 3); (ii) quantify comparative statics that map where coupling remains robust across key drivers, IT utilization, feedstock quality (waste LHV/flow), climate parameterization, and distance-driven thermal decay with parasitic pumping, thereby producing break-even conditions that are directly interpretable for corridor planning (Section 4); and (iii) outline a transparent accounting interface between energy-service substitution and cost-of-computing metrics (LCOC), clarifying what inputs would be required for project-specific evaluation (Section 5), while deliberately avoiding a full lifecycle inventory exercise that is better treated as complementary work. By separating first-order feasibility constraints from second-order component optimization, this paper aims to provide decision-ready siting and scaling criteria for urban AI corridors under grid stress.

## Section II. Integrated System - an Input–Output Black Box

This section introduces the integrated Waste-to-Energy WtE–AIDC concept using an input–output accounting lens. We intentionally abstract from equipment-level engineering (pipe routing, welding, chiller internals, turbine configuration) and focus on the minimum set of energy-service flows that determine feasibility and economic value: waste-derived primary energy, electricity, recoverable heat,

delivered cooling service, grid purchases, and parasitic requirements. Figure 1 provides the system topology and accounting boundary; Figure 2 summarizes the corresponding cascade allocation of waste-derived energy services in the integrated configuration.

### A. System topology, boundary conditions, and the counterfactual benchmark

Figure 1 represents the integrated system as three facility nodes linked by energy-service pathways. The WtE plant converts municipal solid waste  $W$  with heating value  $LHV$  into (i) electricity  $E^{wte}$  and (ii) recoverable thermal energy  $Q^{wte}$ . Electricity can be supplied to the AIDC campus via an on-site connection (or, equivalently, can offset grid purchases). Recoverable heat is routed to a coupling link, which is modeled as a black box that converts heat into cooling through absorption chilling. The coupling link is characterized by three quantities that are sufficient for campus-scale accounting: an absorption performance parameter  $COP_a$ , a distance-dependent thermal delivery factor  $\eta_{tr}(L)$ , and parasitic electricity demand  $W_{par}(L)$  that reflects pumping and auxiliary loads associated with thermal transport and conversion.

The AIDC campus consumes IT power  $P_{IT} = \rho P_{IT}^{\max}$  and requires cooling  $Q_{req} = \gamma P_{IT}$  to deliver compute service  $\mathcal{K}$ . Grid electricity enters the campus at price  $p^e$  as  $E^{\text{grid}}$ , supplying IT load, fixed overhead, and any residual cooling that is not covered by the heat-driven pathway. The dashed connection in Figure 1 denotes the counterfactual standalone benchmark: in the absence of coupling, the campus must meet its cooling requirement via mechanical chilling with coefficient of performance  $COP_m$ , implying a cooling electricity requirement proportional to  $\frac{Q_{req}}{COP_m}$ . In the integrated system, the heat-to-cooling pathway partially or fully displaces this cooling electricity component, creating the physical basis for reductions in purchased electricity and improved operational energy metrics.

Two boundary clarifications are central. First, the figure does not assert a specific engineering layout; it specifies the accounting objects needed to evaluate coupled versus standalone operation. Second, distance  $L$  enters only through deliverability and parasitics,  $\eta_{tr}(L)$  and  $W_{par}(L)$ , so the topology is compatible with a wide range of corridor-scale co-location designs. This is consistent with the paper's objective: to establish the viability and value logic of integrated WtE–AIDC deployments without committing to a single hardware blueprint.

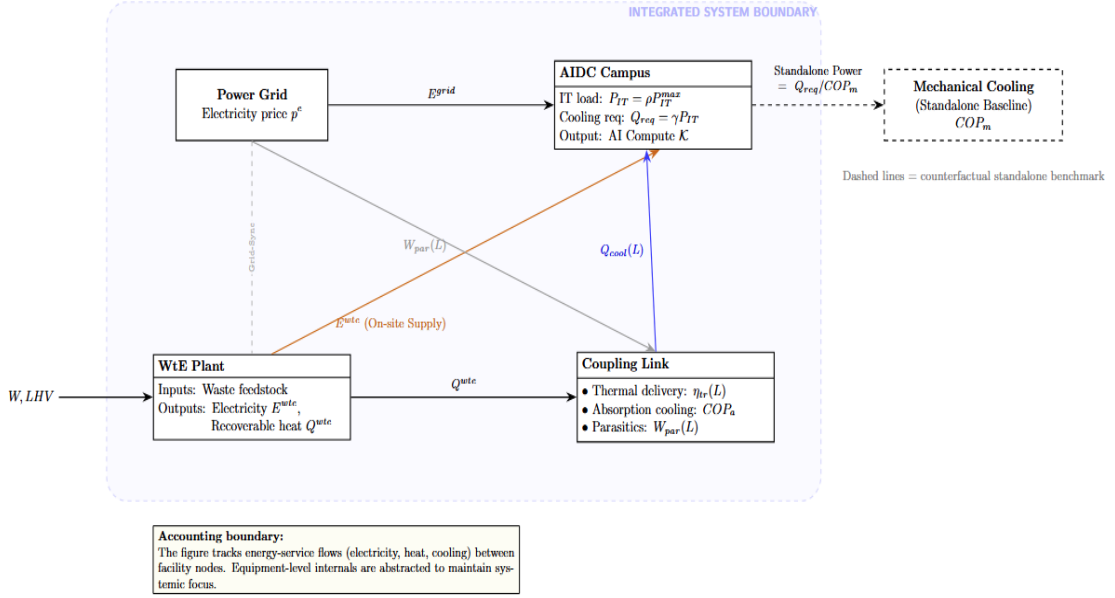
### B. Grade matching and cascade utilization as an accounting principle

While Figure 1 establishes the topology and benchmark, Figure 2 summarizes the central economic–thermodynamic mechanism: grade matching through cascade utilization. A conventional WtE facility is typically evaluated by its electricity output alone, implicitly treating residual heat as a low-value byproduct. In contrast, an AIDC's operational constraint is not only electricity supply but also the continuous provision of cooling to reject heat from computation. The integrated design reassigns the low-grade thermal stream  $Q^{wte}$  to a high-demand service sink, cooling, thereby converting a typically under-utilized output into an electricity-offsetting service.

Figure 2 visualizes this reallocation in energy-service terms. A fixed waste-energy input is partitioned into a high-grade electricity stream (used directly and/or as an offset to grid purchases), a thermal-driven cooling service stream delivered to the AIDC, and a residual loss component labeled as rejected heat and conversion losses. The purpose of the diagram is not to claim universal numerical shares, those depend on site conditions and are explored in later sections, but to clarify the accounting logic: the coupled system

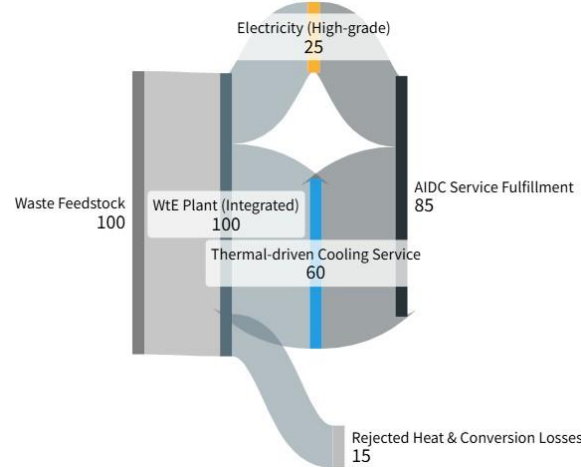
produces a portfolio of useful services (electricity and cooling) from the same primary input, and the cooling service is valuable precisely because it displaces mechanical cooling electricity that would otherwise be purchased from the grid. In this sense, the integrated system can be evaluated as a restructuring of the input–output mapping from waste energy to compute-enabling services, rather than as a marginal improvement to any single component.

Fig. 1. System architecture and energy-service flow topology of the integrated WtE and AI DC synergetic framework.



Notes: The dashed blue perimeter defines the integrated system boundary: MSW is converted to electricity  $E^{wte}$  and recoverable heat  $Q^{wte}$ . The coupling link uses absorption chilling to convert delivered heat into cooling  $Q_{cool}(L)$  with distance-dependent delivery decay  $\eta_{tr}(L)$ ; the grid supplies residual electricity  $E^{grid}$  and parasitic power  $W_{par}(L)$ . The dashed modules on the right depict the standalone baseline in which cooling is met exclusively by electric mechanical chilling ( $COP_m$ ), providing the counterfactual for avoided electricity and PUE impacts.

Fig. 2. Cascade energy accounting and service fulfillment topology of the integrated WtE-AIDC nexus



Notes: Sankey flows report an energy-equivalent balance normalized to 100 units of waste feedstock. Useful delivery to the AIDC combines electricity for IT loads and thermally driven cooling converted from recoverable heat, illustrating grade matching (power from high-grade energy; cooling from low-grade heat). The remaining stream aggregates unrecoverable rejection and conversion losses across the coupled Rankine–absorption pathway.

The two figures jointly discipline the modeling choices that follow. First, the topology in Figure 1 motivates regime-based analysis: the extent to which delivered cooling covers campus cooling requirements determines whether additional heat supply yields marginal electricity savings or whether the system reaches a coverage plateau. Second, the cascade view in Figure 2 motivates quality-adjusted performance comparisons: when a single primary input produces multiple useful services, electricity-only efficiency measures are incomplete, and system-level evaluation must credit the cooling service through an explicit accounting channel. These points guide the thermodynamic boundary conditions and comparative statics introduced in Sections 3–4, where we quantify (i) how coupling changes operational electricity intensity (via PUE-based metrics) and (ii) how feasibility and value depend on feedstock quality and distance-driven thermal decay.

## Section III. Economic–physical model: minimal thermodynamic constraints

This section formalizes a thermoeconomic model for the coupled Waste-to-Energy–AI DC (WtE–AIDC) architecture. The goal is not to resolve equipment-level design, but to impose the minimum physical constraints needed for credible accounting and to define system-consistent performance metrics that can support comparative statics in Section 4.

### A. Notation and Boundary Assumptions

We model all flows as steady-state rates. A dot over a variable denotes a rate (e.g., MW, MJ/s). The integrated system boundary includes (i) the WtE plant converting waste chemical energy into electricity and recoverable heat, (ii) a thermal bridge delivering usable heat to the DC, and (iii) conversion of heat to cooling via absorption chilling.

TABLE I. LIST OF SYMBOLS AND THERMODYNAMIC PARAMETERS

Symbol	Definition	Units
$\dot{m}_w$	Waste mass flow rate	kg/s
LHV	Lower heating value of waste	MJ/kg
$\dot{E}_{in}$	Primary energy input from waste ( $\dot{m}_w \cdot \text{LHV}$ )	MW
$\eta_c$	Effective combustion/boiler utilization efficiency	–
$\eta_e$	Net electrical conversion efficiency (WtE)	–
$\alpha_h$	Recoverable heat fraction of non-electric output (heat recovery factor)	–
$\dot{W}_e$	Net electric output from WtE	MW
$\dot{Q}_h$	Recoverable thermal output available for downstream use	MW
L	Separation distance (WtE to DC) / thermal bridge length	km (or m)
$\eta_{tr}(L)$	Effective thermal delivery factor (reduced-form)	–
$\beta$	Thermal decay coefficient in $\eta_{tr}(L)$	1/km
$\text{COP}_{abs}$	Absorption chiller coefficient of performance	–
$\text{COP}_m$	Mechanical (electric) chiller COP	–
$\dot{Q}_{cool}$	Cooling rate supplied to DC	MW
$\dot{W}_{IT}$	DC IT electrical load	MW
$\gamma$	Cooling requirement per IT load ( $\dot{Q}_{req} = \gamma \dot{W}_{IT}$ )	–
$\dot{W}_{aux}$	Non-cooling auxiliary DC load (fans, UPS losses, lighting)	MW
$\dot{W}_{par}$	Parasitic work for thermal delivery & absorption (pumps, controls)	MW
$T_0$	Ambient reference temperature	K
$T_c$	Chilled-water / refrigeration temperature	K
$\phi_c$	Cooling exergy factor = $\frac{T_0}{T_c} - 1$	–

Our metrics distinguish (a) facility accounting (electric loads at the DC) and (b) system accounting (primary-energy and exergy within the coupled boundary). This prevents “metric gaming” concerns when cooling is heat-driven rather than electricity-driven.

### B. Minimal Energy-Flow Equations

### (1) Waste-to-energy conversion

The primary energy input rate from waste is:

$$\dot{E}_{in} = \dot{m}_w \cdot LHV \quad (1)$$

Net electricity output is modeled as:

$$\dot{W}_e = \eta_e \eta_c \dot{E}_{in} \quad (2)$$

The recoverable thermal output (for downstream utilization):

$$\dot{Q}_h = \alpha_h (\eta_c \dot{E}_{in} - \dot{W}_e) \quad (3)$$

Equation (3) treats heat recovery as a plant-level recoverable fraction of the non-electric useful energy inside the boundary.

### (2) Thermal delivery (spatial feasibility constraint)

Thermal delivery to the DC is constrained by distance  $L$  through a reduced-form delivery factor:

$$\dot{Q}_{del} = \eta_{tr}(L) \dot{Q}_h, \eta_{tr}(L) = \exp(-\beta L) \quad (4)$$

This  $\eta_{tr}(L)$  term compactly captures aggregate thermal losses, imperfect insulation, and operational constraints (including pumping/controls) **without** claiming detailed pipe-network thermohydraulics. It is therefore appropriate for comparative statics and screening-level feasibility.

### (3) Absorption cooling transformation

Delivered heat is converted into cooling via absorption chilling:

$$\dot{Q}_{cool} = COP_{abs} \dot{Q}_{del} \quad (5)$$

The DC's cooling requirement is parameterized as:

$$\dot{Q}_{req} = \gamma \dot{W}_{IT} \quad (6)$$

Define the heat-driven coverage share:

$$f \equiv \min \left\{ 1, \frac{\dot{Q}_{cool}}{\dot{Q}_{req}} \right\} \quad (7)$$

Residual cooling demand  $(1 - f)\dot{Q}_{req}$  is met by mechanical chilling, requiring electricity:

$$\dot{W}_{cool,m} = \frac{(1 - f)\dot{Q}_{req}}{COP_m} \quad (8)$$

Finally, parasitic work  $\dot{W}_{par}$  (pumps, controls, circulation) is modeled as a transparent reduced-form load:

$$\dot{W}_{par} = \kappa_0 + \kappa_1 \dot{W}_{IT} + \kappa_2 L \quad (9)$$

where  $\kappa_0, \kappa_1, \kappa_2$  can be scenario-calibrated. This keeps the model auditable while preserving the focus on system accounting.

## C. System-Consistent Performance Metrics

### (1) Extended PUE - auditable under heat-driven cooling

Conventional PUE is electricity-only and becomes non-comparable once cooling is supplied thermally. We therefore define two complementary metrics:

(i) Electric PUE (facility electricity only):

$$PUE_{elec} \equiv \frac{\dot{W}_{IT} + \dot{W}_{aux} + \dot{W}_{cool,m} + \dot{W}_{par}}{\dot{W}_{IT}} \quad (10)$$

This metric answers: How much grid electricity does the DC draw per unit IT load under coupling?

(ii)  $PUE_{sys}$  (within the coupled boundary), a system-boundary accounting ratio that is conceptually aligned with an Energy-Service Intensity (ESI) in that it maps IT load to the total energy burden required to deliver computing and cooling services within the coupled system boundary. We retain the notation  $PUE_{sys}$  for consistency with the paper's derivations, but emphasize that it is not ISO/IEC PUE and is not intended for cross-study PUE benchmarking; it is introduced solely to ensure conservation-consistent bookkeeping when cooling is supplied through non-electric energy services.

$$PUE_{sys} \equiv \frac{\dot{W}_{IT} + \dot{W}_{aux} + \dot{W}_{cool,m} + \dot{W}_{par} + \dot{Q}_{del}}{\dot{W}_{IT}} \quad (11)$$

Here  $\dot{Q}_{del}$  is counted as an energy input supporting computing, ensuring comparability across electricity-driven and heat-driven cooling. This avoids the critique that PUE improves simply because energy is shifted from electricity to heat.  $PUE_{elec}$  captures grid capacity relief and electric OpEx;  $PUE_{sys}$  captures total energy intensity within the integrated system boundary.

(2) *Systemic Exergy Efficiency* ( $\eta_{ex}$ )

Energy quantities alone do not distinguish high-grade electricity from low-grade heat. We therefore define a systemic exergy efficiency, treating waste chemical energy as the primary exergy input (a standard screening approximation for comparative statics):

$$Ex_{in} \equiv \eta_c \dot{E}_{in} \quad (12)$$

Useful exergy output includes electricity and the exergy of delivered cooling. The exergy of a cooling effect at temperature  $T_c$  relative to ambient  $T_0$  is:

$$\phi_c \equiv \frac{T_0}{T_c} - 1, Ex_{cool} \equiv \phi_c \dot{Q}_{cool} \quad (13)$$

Thus total useful exergy output is:

$$Ex_{out} \equiv \dot{W}_e + Ex_{cool} \quad (14)$$

Define systemic exergy efficiency:

$$\eta_{ex} \equiv \frac{Ex_{out}}{Ex_{in}} = \frac{\dot{W}_e + \phi_c \dot{Q}_{cool}}{\eta_c \dot{E}_{in}} \quad (15)$$

$\eta_{ex}$  is a quality-adjusted utilization index, which increases when low-grade heat is converted into a service (cooling) that offsets high-value electricity use, i.e., when the system reduces exergy destruction through better grade matching.

## D. A sufficient condition for thermoeconomic superiority (Proposition)

Holding  $\dot{W}_{IT}$  fixed, a sufficient condition for the coupled system to weakly dominate the standalone architecture in systemic exergy utilization is:

$$\phi_c \dot{Q}_{cool} \geq \dot{W}_{par} \quad (16)$$

Substituting (4)–(5), this becomes:

$$\phi_c \text{COP}_{abs} \eta_{tr}(L) \dot{Q}_h \geq \dot{W}_{par} \quad (17)$$

Proof sketch (intuition): In the standalone case, recoverable heat  $\dot{Q}_h$  is predominantly rejected, contributing no useful exergy output. Under coupling, the same heat is converted into cooling whose exergy content is  $\phi_c \dot{Q}_{cool}$ . The coupled system improves exergy utilization whenever this quality-adjusted cooling contribution exceeds the additional parasitic work required to deliver and convert the heat. A formal derivation is straightforward from (12)–(15) and is provided in Appendix A.

## Section IV. Simulation Design and Comparative Statics

This section quantifies the operational and thermoeconomic implications of integrating a waste-to-energy (WtE) plant with an AI DC (AIDC) through a heat-driven cooling pathway. The simulations are intentionally “minimum-physics, maximum-accountability”: we impose conservation-consistent thermodynamic boundaries and parameterize only the margins that govern feasibility and value, IT load utilization, feedstock quality, and spatial heat-delivery constraints. Figures 1 and 2 summarize the baseline performance and quality-adjusted efficiency gains; Figures 5 and 6 provide comparative statics on (i) waste heating value and (ii) distance-driven thermal decay and parasitic requirements.

This paper is a design proposal and screening framework, not a site-specific engineering feasibility study. We therefore do not calibrate the model to a particular city or facility, because such calibration would require project-specific details that are beyond the present contribution and would not generalize. Instead, we anchor all first-order drivers (thermal decay, pumping parasitics, and absorption performance) to published ranges and report conservative–baseline–aggressive scenario packages (Appendix C). The results should be interpreted as order-of-magnitude feasibility bounds and break-even frontiers for corridor planning, which are the appropriate decision object at the pre-design stage.

Before presenting the full comparative statics, we provide a reference configuration to make the framework operationally transparent. The goal is not to claim a site-specific feasibility result, but to show, using a single mid-point parameter set anchored to Appendix C, how the model maps observable inputs (WtE exportable heat, absorption performance, distance-driven decay, and parasitic pumping) into the paper’s planning objects: net avoided cooling electricity and a coverage-defined break-even corridor length. This illustrative configuration is deliberately non-site-specific and should be interpreted as an order-of-magnitude demonstration of the accounting logic that underlies Figures 3–6.

### Representative configuration (illustrative, non-site-specific)

To demonstrate how the framework is used without claiming a specific deployment, we report one representative parameter set drawn from the midpoint of Appendix C and compute the implied break-even corridor length and avoided-electricity magnitude. This reference configuration is not a real project and is provided solely as a transparent illustration of model inputs and outputs.

Thermal supply (representative WtE export stream). Consider a modern regulated WtE facility with MSW lower heating value  $LHV_{MSW} = 10\text{MJ/kg}$  and throughput  $\dot{m}_{MSW} = 1500\text{t/day}$ . The chemical

energy input is 15,000GJ/day. With a net exportable thermal fraction  $\eta_{\text{th,export}} = 0.45$ , the available driving heat at the coupling boundary is  $Q_{\text{drive},0} = 15,000 \times 0.45/86,400 \approx 78.1 \text{ MW}_{\text{th}}$ .

Corridor delivery and cooling conversion. Using the midpoint corridor decay  $\beta = 0.005 \text{ km}^{-1}$ , delivered driving heat at distance  $L$  is  $Q_{\text{drive,del}}(L) = Q_{\text{drive},0} \exp(-\beta L)$ . With a single-effect absorption COP  $COP_{\text{abs}} = 0.75$ , delivered cooling is  $Q_{\text{cool}}(L) = COP_{\text{abs}} Q_{\text{drive,del}}(L) \approx 58.6 \exp(-0.005L) \text{ MW}_{\text{cool}}$ .

Avoided electricity (screening-level). To express cooling service in electric-equivalent terms, we use a baseline electric chiller coefficient of performance  $COP_e = 5$  (i.e., 1MW<sub>e</sub> produces 5MW<sub>cool</sub>), purely as an illustrative conversion factor. The gross avoided electricity associated with  $Q_{\text{cool}}(L)$  is

$$W_{\text{avoid,gross}}(L) = \frac{Q_{\text{cool}}(L)}{COP_e} \approx 11.7 \exp(-0.005L) \text{ MW}_e.$$

Accounting for pumping electricity  $e_{\text{pump}} = 6 \text{ kWh}_e / \text{MWh}_{\text{th}}$  and auxiliary electric-equivalent fraction  $\alpha_{\text{aux}} = 4\%$ , the net avoided electricity is approximated by

$$W_{\text{avoid,net}}(L) \approx \underbrace{11.7}_{\text{gross}} - \underbrace{0.006 \times 78.1}_{\text{pumping}} - \underbrace{0.04 \times 58.6}_{\text{aux}} \exp(-0.005L) \approx 8.9 \exp(-0.005L) \text{ MW}_e.$$

This implies a screening-level magnitude of roughly 8.9 MW<sub>e</sub> net avoided cooling electricity at  $L = 0$ , declining to 8.0 MW<sub>e</sub> at  $L = 20 \text{ km}$  and 7.3 MW<sub>e</sub> at  $L = 40 \text{ km}$ .

Break-even corridor length (coverage-defined). Define a representative AIDC with IT power  $P_{\text{IT}} = 40 \text{ MW}$  and baseline cooling electricity share of 20% of IT power (i.e.,  $W_{\text{cool,base}} = 8 \text{ MW}_e$ ); this “cooling share” is an illustrative bookkeeping assumption used only to define a coverage target. The break-even corridor length  $L^*$  is the distance at which the coupled system can fully cover the baseline cooling electricity demand:  $W_{\text{avoid,net}}(L^*) = W_{\text{cool,base}}$ .

Using  $W_{\text{avoid,net}}(L) \approx 8.9 \exp(-0.005L)$ , we obtain  $L^* \approx \frac{-\ln(\frac{8}{8.9})}{0.005} \approx 21 \text{ km}$ . This illustrates the paper’s planning object: given literature-anchored performance bands (Appendix C), the framework yields a transparent break-even corridor frontier, which can be tightened or shifted once project-specific hydraulic design and dispatch constraints are available.

We stop at the screening and corridor-planning level. A project-calibrated case study would require location-specific routing, diameter optimization, hydraulic station placement, dispatch constraints of the WtE plant, and permitting/community constraints that are not generalizable and are outside the contribution of a first framework paper. Instead, we address external validity by (i) anchoring all first-order drivers to published ranges and reporting conservative–baseline–aggressive packages (Appendix C), and (ii) showing that the break-even frontier is governed by a small set of interpretable parameters,  $\beta$ ,  $COP_{\text{abs}}$ , and pumping/auxiliary parasitics, that can be replaced by any project team once a candidate corridor is identified. With this scope and reference magnitude in place, we now formalize the baseline screening parameterization and accounting identities (Section IV-A), then trace their implications for utilization-dependent PUE effects (IV-B), system-level quality-adjusted efficiency (IV-C), and the key comparative statics in feedstock quality and corridor distance (IV-D–IV-E).

## A. Baseline configuration and screening parameterization

We consider a representative AIDC with maximum IT capacity  $P_{IT}^{\max}$  and utilization  $\rho \in (0,1]$ , so that  $P_{IT} = \rho P_{IT}^{\max}$ . The cooling requirement is modeled as proportional to IT load,  $Q_{req} = \gamma P_{IT}$ , where  $\gamma$  captures site and design conditions. In the standalone benchmark, cooling is supplied electrically via mechanical chillers with coefficient of performance  $COP_m$ . In the integrated configuration, recoverable WtE thermal output drives an absorption chiller with  $COP_a$ , delivered through a heat-transport link with exponential decay  $\eta_{tr}(L) = \exp(-\beta L)$ , where  $L$  is the separation distance and  $\beta$  is an effective thermal attenuation rate.

Let  $Q_{cool}(L)$  denote the delivered cooling potential from WtE heat at distance  $L$ . Define the thermal coverage ratio  $f(L) \equiv \min\left\{1, \frac{Q_{cool}(L)}{Q_{req}}\right\}$ , so that the remaining fraction  $(1-f)$  of cooling demand must be met by mechanical chilling. Facility-level parasitic loads are summarized by a compact reduced-form term  $W_{par}(L)$ , capturing pumps, controls, and distribution losses that scale with system size and, potentially, distance. This representation preserves the key accounting identity for electric demand while avoiding engineering over-specification.

## B. PUE implications across IT load utilization

Figure 3 reports derived PUE as a function of IT load utilization. In the standalone benchmark, PUE exceeds unity because cooling power scales with IT load at rate  $\frac{1}{COP_m}$ , and fixed overheads create a disproportionate burden at low utilization. In the integrated system, delivered cooling is predominantly thermal; the residual electric burden is limited to parasitic loads and fixed overhead. Two implications follow.

First, the coupled configuration produces a lower PUE at all utilization levels considered, indicating that heat-driven cooling can reduce the marginal electricity intensity of computing even when generation efficiency in the WtE plant is not altered. Second, the PUE gap between standalone and coupled configurations is structurally bounded: once  $f(L) = 1$  (full thermal coverage), additional heat availability does not further reduce electric cooling demand, and PUE becomes governed by fixed overhead plus parasitics relative to IT load. This “coverage-induced plateau” is a recurring feature in subsequent sensitivity results.

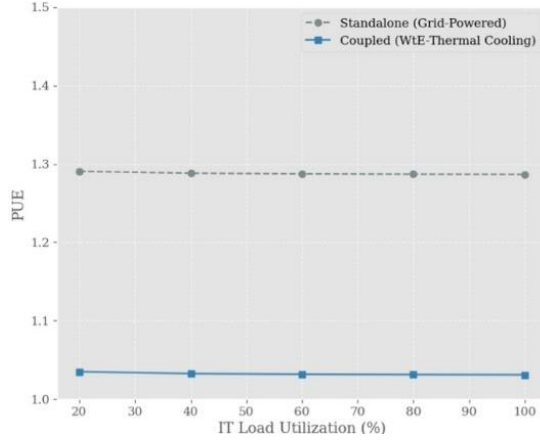
## C. System-level quality-adjusted efficiency

Electricity-only efficiency is an incomplete welfare proxy for integrated energy-computing systems because the coupled configuration produces two valuable outputs: electricity and cooling (which offsets electricity that would otherwise be purchased for cooling). Figure 4 therefore evaluates systemic efficiency using a quality-adjusted accounting in which cooling is credited by an exergy factor that reflects its thermodynamic “grade” relative to ambient conditions. Specifically, the integrated system’s useful output includes both generated electric power and the exergy-equivalent of delivered cooling, while the baseline WtE benchmark credits only electricity generation.

Figure 4 shows that the integrated configuration attains higher systemic efficiency than the electricity-only WtE benchmark. The mechanism is grade matching: WtE’s non-electric thermal output is low-grade relative to electricity but is well matched to the low-grade cooling demand of an AIDC campus. Converting heat to cooling therefore recovers economically valuable services from an energy stream that would otherwise be dissipated or under-utilized. Importantly, the improvement does not rely on optimistic

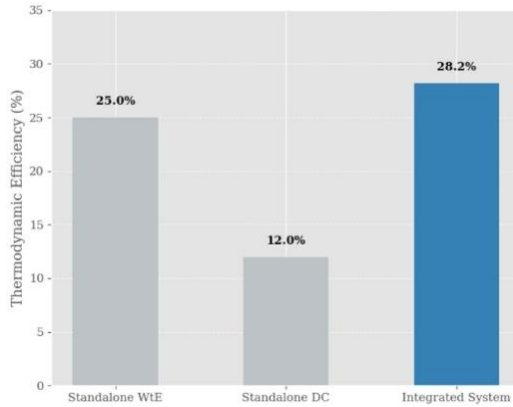
assumptions about generation performance; it arises from reallocating the same primary energy input into a more appropriate output portfolio.

Fig. 3. Performance sensitivity of PUE under variable IT load utilization: A comparative analysis of standalone and coupled architectures.



**Notes:** Electric PUE is plotted against IT utilization for the standalone (grid-powered mechanical cooling) and coupled (WtE heat-driven cooling) configurations. Under the reference parameterization, the coupled system reduces non-IT electricity by substituting absorption-driven cooling for compressor work; the resulting PUE is therefore close to unity. In Fig. 3a we hold  $(W_{aux}/W_{IT})$  and  $(W_{par}/W_{IT})$  constant to isolate the grade-matching channel; relaxing this assumption yields the sensitivity band in Fig. 3b (Table A1 / Appendix C).

Fig. 4. Comparative thermodynamic analysis of systemic exergy efficiency across standalone and integrated operational regimes.



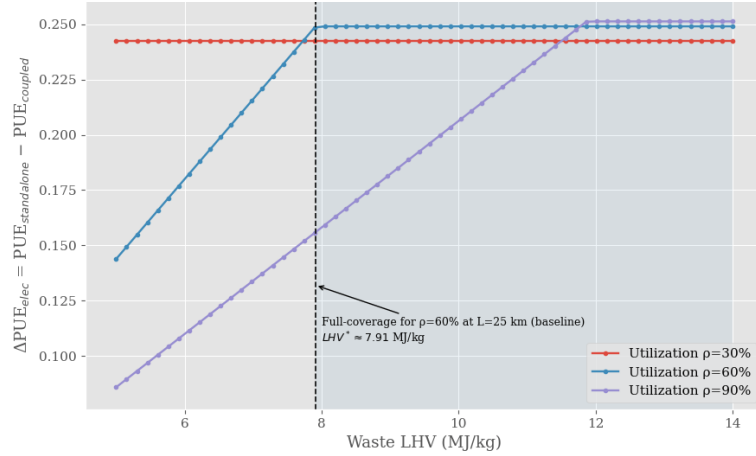
**Notes:** The standalone baseline (mechanical chilling) yields an approximately constant electric PUE of  $\sim 1.29$  over the utilization range shown, while the coupled configuration yields  $\sim 1.03$  under the reference parameterization due to heat-driven cooling and reduced compressor electricity. Fig. 3a holds  $(W_{aux}/W_{IT})$  and  $(W_{par}/W_{IT})$  constant; Fig. 3b relaxes this assumption and reports the resulting sensitivity band (Table A1 / Appendix C).

#### D. Feedstock sensitivity: $\Delta PUE_{elec}$ vs waste LHV

Figure 5 examines how the electric PUE gain,  $\Delta PUE_{elec} \equiv PUE_{standalone} - PUE_{coupled}$ , responds to feedstock lower heating value (LHV) under a fixed separation distance  $L = 25\text{km}$ . Three utilization levels illustrate how load scale interacts with thermal supply.

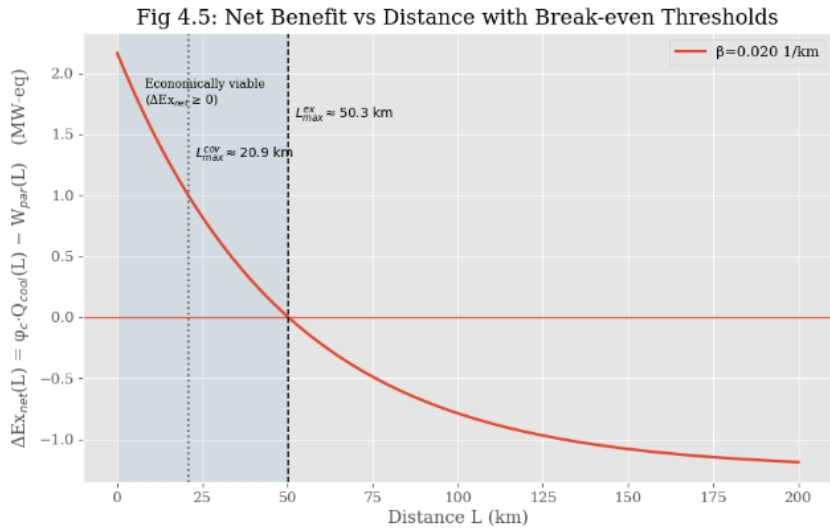
Two patterns are robust. First,  $\Delta\text{PUE}_{\text{elec}}$  is increasing in LHV in the partial-coverage region: higher-LHV waste increases available recoverable heat, raising  $Q_{\text{cool}}(L)$  and thereby increasing  $f(L)$ . This reduces the electrically-driven share of cooling and lowers total facility electricity per unit IT. Second,  $\Delta\text{PUE}_{\text{elec}}$  flattens once the system reaches full thermal coverage for the utilization scenario in question. The reference-case threshold  $\text{LHV}^* \approx 7.91 \text{ MJ/kg}$  for  $\rho = 60\%$  marks the point at which delivered absorption cooling meets the modeled cooling requirement; beyond this point, additional feedstock quality does not further reduce electric cooling demand, and gains are limited by parasitic and fixed overhead components.

Fig. 5. Cooling Coverage and Electricity Displacement under Feedstock Variability: Sensitivity to Waste LHV and Throughput



**Notes:** Comparative statics vary MSW feedstock conditions (LHV and throughput) to compute recoverable WtE heat and the resulting delivered cooling, translated into electric-equivalent displacement of baseline mechanical chilling in the standalone benchmark. Cooling coverage is defined as the share of the AIDC cooling requirement met by the heat-to-cooling pathway after delivery decay and auxiliary/parasitic electricity are accounted for. All other parameters follow the reference case (Sections 3–4); gains scale approximately with feedstock below full coverage and saturate once coverage reaches unity.

Fig. 6. Net Benefit versus Corridor Distance: Thermal-Delivery Decay, Parasitic Work, and the Break-Even Radius for WtE–AIDC Coupling



**Notes:** Net operational benefit is plotted against WtE–AIDC separation distance  $L$ , combining distance-dependent delivery decay  $\eta_{tr}(L)$  (which reduces delivered cooling) and parasitic electricity  $W_{par}(L)$  (which increases with transport and auxiliaries). The break-even distance is defined by the zero crossing where avoided baseline cooling electricity equals parasitic electricity cost under the reference parameterization (Sections 3–4 / Appendix C). The resulting curve provides a screening siting rule: coupling is attractive within the break-even range and becomes increasingly fragile as distance increases.

The dependence on utilization is economically meaningful. Higher utilization requires a larger absolute cooling load, so full coverage is harder to achieve; as a result, the  $\rho = 90\%$  curve exhibits a longer increasing segment before reaching its plateau. Conversely, the  $\rho = 30\%$  scenario remains fully covered over the plotted LHV range under baseline assumptions, implying that marginal improvements in waste quality deliver limited incremental electric savings once coverage is already complete.

## E. Spatial feasibility and break-even distances

While feedstock quality governs thermal supply, spatial separation governs deliverability. Figure 6 characterizes distance constraints using a net exergy-benefit function,  $\Delta Ex_{net}(L) \equiv \phi_c Q_{cool}(L) - W_{par}(L)$ , where  $\phi_c$  is the exergy factor associated with cooling at the chilled-water condition. The exponential decay in  $\eta_{tr}(L)$  reduces delivered cooling with distance, while parasitics represent the electric cost of maintaining thermal transport and system operation.

Two thresholds emerge. The “coverage threshold”  $L_{max}^{cov} \approx 20.9\text{km}$  is the largest distance at which delivered absorption cooling can fully cover the modeled cooling requirement ( $f(L) = 1$ ) in the reference configuration. Beyond  $L_{max}^{cov}$ , the system transitions to partial coverage, and mechanical chilling is required for the residual cooling demand. The “thermoeconomic break-even”  $L_{max}^{ex} \approx 50.3\text{km}$  is the largest distance at which the quality-adjusted cooling benefit remains non-negative after accounting for parasitic electricity. For  $L \leq L_{max}^{ex}$ , the coupled system is thermoeconomically viable in the sense that recovered cooling exergy weakly dominates its parasitic burden; for  $L > L_{max}^{ex}$ , attenuation and parasitics overwhelm the recovered value, and the coupling ceases to be justified on the modeled terms.

These thresholds provide a compact siting implication: co-location or corridor-scale adjacency is not merely convenient but is often necessary for the coupling to deliver meaningful economic value. The results also clarify why distance is the central realism constraint in an otherwise favorable grade-matching environment, without short thermal links (or equivalently, without sufficiently low  $\beta$  and parasitic intensity), recoverable heat cannot be monetized as reliable cooling services.

Across the four figures, three messages are consistent. First, coupling reduces electric intensity of computing (Figure 1) and improves system-level quality-adjusted efficiency (Figure 4) through grade matching. Second, the magnitude of PUE gains is governed by whether the system is in a partial-coverage or full-coverage regime; this produces observable plateaus in  $\Delta PUE_{elec}$  once thermal coverage is achieved (Figure 5). Third, spatial decay creates hard feasibility boundaries, summarized by coverage and break-even distances (Figure 6), which translate the thermodynamic logic into actionable siting constraints. Together, these results motivate the subsequent discussion of levelized computing cost and strategic valuation under realistic corridor-scale deployments.

## Section V. Financial and Strategic Implications

This section translates the comparative-statics results into decision-relevant objects that can be evaluated with standard accounting inputs. The aim is deliberately modest: rather than building a full

project-finance model with a detailed capital structure, we provide a computable prototype for valuing coupled WtE–AIDC deployments and a disciplined ESG framing that specifies mechanisms and measurement boundaries without over-claiming precision.

### A. A computable prototype for the LCOC

Cost comparisons for AI DCs are typically reported in incompatible units, \$/kWh for electricity procurement, \$/ton for waste services, \$/MW for capacity, and PUE for operational efficiency, making integrated designs difficult to evaluate on a common scale. To align valuation with the object ultimately demanded by buyers and planners, we define a Levelized Cost of Computing (LCOC) as the discounted cost of providing computing service divided by the discounted quantity of computing delivered:  $LCOC \equiv$

$\frac{\sum_{t=0}^T c_t (1+r)^{-t}}{\sum_{t=0}^T \mathcal{K}_t (1+r)^{-t}}$ . Here  $C_t$  collects all costs and net revenues attributable to the integrated campus in period  $t$ , and  $\mathcal{K}_t$  is a measurable compute-service index. In practice,  $\mathcal{K}_t$  can be selected to match data availability and the intended audience. A conservative accounting choice is  $\mathcal{K}_t = E_t^{IT}(\text{MWh}_{IT})$ , which yields  $\frac{\$}{\text{MWh}_{IT}}$  and harmonizes directly with PUE-based reporting. When telemetry is available,  $\mathcal{K}_t$  may instead represent accelerator-hours or normalized workload units (e.g., tokens), enabling comparisons across hardware generations and scheduling regimes.

The value of LCOC lies in how it internalizes the coupling channels identified in Section 4. A parsimonious decomposition writes total cost as the sum of (i) computing and coupling capital expenditures, (ii) operating and maintenance costs, (iii) the net cost of purchased electricity, and (iv) the net cost of waste services, allowing for any electricity export revenues where applicable:

$$C_t = \text{CapEx}_t^{IT} + \text{CapEx}_t^{\text{couple}} + \text{OpEx}_t^{IT} + p_t^e E_t^{\text{grid}} + p_t^w W_t - \text{Rev}_t^{\text{elec}} \quad (18)$$

The key object affected by the WtE–cooling linkage is  $E_t^{\text{grid}}$ , the electricity purchased from the grid. Using the coverage formulation in Section 4, grid electricity can be represented as IT electricity plus overhead and parasitics, plus the residual mechanical-cooling requirement after thermal coverage is credited:

$$E_t^{\text{grid}} = E_t^{IT} + E_t^{\text{aux}} + (1 - f(L)) \frac{Q_{\text{req},t}}{\text{COP}_m} + W_{\text{par},t}(L) - E_t^{\text{on-site}} \quad (19)$$

This expression makes explicit why Figures 5-6 are financially informative rather than merely technical. Feedstock quality (through recoverable heat) and utilization (through  $Q_{\text{req},t} \propto P_{IT,t}$ ) determine whether the system operates in a partial-coverage regime or reaches full coverage; once full coverage is achieved, marginal changes in LHV do not materially reduce grid electricity further, and LCOC becomes dominated by parasitics, overhead, and the price path  $p_t^e$ . Distance enters through the attenuation of deliverable cooling and the parasitic burden; beyond the break-even distance implied by  $\Delta \text{Ex}_{\text{net}}(L)$ , the coupling channel ceases to reduce net cost, so LCOC screening should treat such sites as fundamentally different projects rather than extrapolations of the co-located case.

Viewed this way, LCOC is a practical screening statistic: it can be estimated with a thin but auditable dataset, electricity prices, waste-service terms, utilization, baseline cooling efficiency, absorption performance, and the distance-governed coverage schedule, while remaining consistent with the thermodynamic constraints that discipline the engineering side of the model.

## B. Strategic implications: corridor economics and capacity-constrained deployment

The comparative statics imply that WtE–AIDC integration is best interpreted as a corridor strategy rather than a universal design rule. The distance thresholds in Figure 6 identify a narrow set of siting conditions under which low-grade heat can be monetized as reliable cooling services at scale. Within this window, the integrated design generates value through capacity relief as much as through unit-cost reduction. When grid interconnection is binding, reducing electricity for cooling increases deliverable IT output per unit of grid capacity, effectively relaxing a key deployment constraint without requiring commensurate expansion of transmission or on-site generation. This mechanism is particularly relevant in regions where AIDC buildouts are limited by interconnection queues and local thermal footprints, because the marginal value of “freed” grid MW can exceed the direct energy-cost savings.

The same structure also clarifies expansion logic. Because thermal deliverability degrades with distance, incremental campus expansion that increases the effective separation between the thermal source and new IT halls can move the system discontinuously from full coverage to partial coverage, or from viability to non-viability. The thresholds  $L_{\max}^{\text{cov}}$  and  $L_{\max}^{\text{ex}}$  therefore provide a disciplined rule for phase planning: additions that push the campus beyond these boundaries should be evaluated as requiring a new thermal node, an alternative cooling architecture, or a different energy contract, rather than being priced as marginal capacity on the original cost curve.

Finally, the coupled system naturally spans multiple counterparties, municipal waste contracts, electricity offtake or market exposure, and compute demand, creating the possibility of cash-flow diversification. While a full contracting analysis is outside this paper, the LCOC decomposition highlights where the contractual boundaries matter most: pass-through clauses for electricity price risk, the structure of tipping fees and gate revenues, and the assignment of responsibilities for parasitic and distribution losses that grow with distance.

## C. ESG mechanisms and measurement boundaries

The ESG relevance of WtE–AIDC coupling follows from mechanisms that are conceptually straightforward but often reported without transparent boundaries. We emphasize two channels and specify measurement hooks that can be used for disciplined reporting, leaving full lifecycle quantification to subsequent work.

First, diverting municipal solid waste from landfills to WtE changes the counterfactual methane pathway. The operational object that the project controls is the quantity and composition of waste diverted,  $W_t$ , and the appropriate accounting practice is to pair this with an explicit counterfactual (e.g., landfilling under a specified methane capture regime). A defensible empirical approach is therefore to report diversion volumes and apply standardized emissions factors from regulated inventories or established protocols as a sensitivity range, rather than asserting a single precise methane abatement number.

Second, the coupling reduces the electricity intensity of computing by lowering the share of cooling supplied by mechanical chillers. This is directly measurable through operational energy metrics such as  $\Delta\text{PUE}_{\text{elec}}$  under stated utilization, LHV, and distance conditions, and through normalized electricity intensity  $\frac{E_t^{\text{grid}}}{K_t}$  using the same compute-service denominator chosen for LCOC. Importantly, Figures 5-6 imply that such improvements are regime-dependent: the claimable efficiency benefit must be conditioned

on whether the system is in full coverage, partial coverage, and within the identified viability distance window.

We note that a full LCOC implementation requires project-specific CAPEX/OPEX data (pipeline routing and diameter choice, pumping station placement, maintenance, water treatment, thermal dispatch constraints, and financing terms). These details are intentionally abstracted here to keep the paper at the screening level. In follow-on work, we will operationalize the LCOC module by incorporating (i) a standardized CAPEX library for district thermal networks and absorption equipment, (ii) OPEX components including parasitic electricity, water and chemical treatment, and maintenance, and (iii) dispatch/availability constraints for the WtE heat stream. The present paper's contribution is to define the conservation-consistent boundary and break-even frontier that such an LCOC evaluation must respect.

Taken together, these ESG channels suggest a reporting template that is both credible and compatible with later lifecycle work: disclose (i) waste diversion volumes and the counterfactual treatment path, (ii) operational electricity intensity of computing and its dependence on utilization and distance, and (iii) the boundary conditions used to translate thermal coupling into avoided grid electricity. This approach preserves the core strategic message, grade matching can jointly improve operational efficiency and shift the emissions profile, without relying on brittle full-lifecycle estimates that are better handled in more specialized follow-on analyses.

## Conclusions

This paper reframes WtE–data-center integration as an energy-service substitution problem governed by grade matching, rather than an equipment novelty claim. Modeling the coupled WtE–AIDC topology as an input–output accounting “black box” with a transparent standalone benchmark, we show how recoverable WtE heat can be converted into delivered cooling via absorption, thereby displacing electricity that would otherwise be consumed by mechanical chilling.

The screening results imply that thermoeconomic value is governed by three first-order determinants: (i) cooling coverage of the IT heat load, (ii) parasitic electricity for transport and auxiliaries, and (iii) distance-driven delivery decay. These determinants generate a break-even corridor frontier: coupling is attractive within a limited radius and becomes fragile once attenuation and parasitics push the system into partial coverage or negative net benefit. Sensitivities to utilization and feedstock quality primarily operate through the same regime logic, producing a predictable plateau once full coverage is achieved.

To connect engineering-accounting gains to decision language, we outline a computable interface to Levelized Cost of Computing (LCOC) and an ESG reporting boundary based on measurable mechanisms (waste diversion counterfactuals and electricity-intensity changes), while intentionally stopping short of full lifecycle inventories and site-specific hydraulic design. Overall, the framework provides siting-ready feasibility conditions and interpretable break-even thresholds for corridor planning of WtE–AIDC co-location under grid stress.

## References

- [1] International Energy Agency (IEA), *Energy and AI*. Paris, France: IEA, 2025. [Online]. Available: <https://www.iea.org/reports/energy-and-ai>
- [2] A. Shehabi *et al.*, *2024 United States Data Center Energy Usage Report*. Berkeley, CA, USA: Lawrence Berkeley National Laboratory, 2024. (Rep. No. LBNL-2001594). [Online]. Available: <https://eta.lbl.gov/publications/2024-united-states-data>
- [3] M. Azarifar *et al.*, “Liquid cooling of data centers: A necessity facing challenges,” *Applied Thermal Engineering*, vol. 247, Art. no. 123112, 2024. doi: 10.1016/j.applthermaleng.2024.123112. [Online]. Available: <https://doi.org/10.1016/j.applthermaleng.2024.123112>
- [4] IPCC, “Summary for Policymakers,” in *Climate Change 2021: The Physical Science Basis* (Contribution of Working Group I to the Sixth Assessment Report of the Intergovernmental Panel on Climate Change). Cambridge, U.K.: Cambridge University Press, 2021. [Online]. Available: <https://www.ipcc.ch/report/ar6/wg1/>
- [5] United Nations Environment Programme (UNEP) and Climate and Clean Air Coalition (CCAC), *Global Methane Assessment: Benefits and Costs of Mitigating Methane Emissions*. Nairobi, Kenya: UNEP, 2021. [Online]. Available: <https://www.unep.org/resources/report/global-methane-assessment-2021>
- [6] Q. He and C. Qu, “Modular Landfill Remediation for AI Grid Resilience,” *arXiv*, arXiv:2512.19202, Dec. 2025. doi: 10.48550/arXiv.2512.19202. [Online]. Available: <https://arxiv.org/abs/2512.19202>
- [7] European Commission, “Commission Implementing Decision (EU) 2019/2010 of 12 November 2019 establishing the best available techniques (BAT) conclusions, under Directive 2010/75/EU, for waste incineration,” *Official Journal of the European Union*, L312, Dec. 3, 2019. [Online]. Available: [https://eur-lex.europa.eu/eli/dec\\_impl/2019/2010/oj](https://eur-lex.europa.eu/eli/dec_impl/2019/2010/oj)
- [8] U.S. Environmental Protection Agency, “Large Municipal Waste Combustors (LMWC): New Source Performance Standards (NSPS) and Emissions Guidelines,” EPA, updated Apr. 15, 2025. [Online]. Available: <https://www.epa.gov/stationary-sources-air-pollution/large-municipal-waste-combustors-lmwc-new-source-performance>
- [9] Ministry of Ecology and Environment of the People’s Republic of China, “Standard for pollution control on the municipal solid waste incineration (GB 18485-2014),” effective Jul. 1, 2014. [Online]. Available: [https://english.mee.gov.cn/Resources/standards/Solid\\_Waste/SW\\_control/201603/t20160303\\_331143.shtml](https://english.mee.gov.cn/Resources/standards/Solid_Waste/SW_control/201603/t20160303_331143.shtml)
- [10] L. Tang, J. Guo, R. Wan, M. Jia, J. Qu, L. Li, and X. Bo, “Air pollutant emissions and reduction potentials from municipal solid waste incineration in China,” *Environmental Pollution*, vol. 319, Art. no. 121021, 2023. doi: 10.1016/j.envpol.2023.121021. [Online]. Available: <https://doi.org/10.1016/j.envpol.2023.121021>
- [11] ISO/IEC, *ISO/IEC 30134-2:2016, Information technology, Data centres, Key performance indicators, Part 2: Power Usage Effectiveness (PUE)*. Geneva, Switzerland: ISO, 2016. [Online]. Available: <https://www.iso.org/standard/63451.html>
- [12] X. Yuan *et al.*, “Waste heat recoveries in data centers: A review,” *Renewable and Sustainable Energy Reviews*, vol. 188, Art. no. 113777, 2023. [Online]. Available: <https://research.aalto.fi/en/publications/waste-heat-recoveries-in-data-centers-a-review/>

- [13] Y. Wang *et al.*, “Data center integrated energy system (DC-IES): A multiphysical design and optimal operation framework,” *The Innovation Energy*, 2024. [Online]. Available: <https://www.sciencedirect.com/science/article/pii/S2949854624000012>
- [14] M. Ibrahim *et al.*, “Absorption refrigeration systems integrated with thermal energy storage: A review of performance, modelling and control strategies,” *Journal of Energy Storage*, 2024. [Online]. Available: <https://www.sciencedirect.com/>
- [15] G. Tsatsaronis, “Thermoeconomic analysis and optimization of energy systems,” *Progress in Energy and Combustion Science*, vol. 19, no. 3, pp. 227–257, 1993. doi: 10.1016/0360-1285(93)90016-8. [Online]. Available: [https://doi.org/10.1016/0360-1285\(93\)90016-8](https://doi.org/10.1016/0360-1285(93)90016-8)
- [16] A. Lazzaretto and G. Tsatsaronis, “SPECO: A systematic and general methodology for calculating efficiencies and costs in thermal systems,” *Energy*, vol. 31, nos. 8–9, pp. 1257–1289, 2006. doi: 10.1016/j.energy.2005.03.011. [Online]. Available: <https://doi.org/10.1016/j.energy.2005.03.011>

## Appendix A. Proof of Proposition 1 (A Sufficient Condition for Thermo-economic Superiority)

This appendix provides a formal derivation of Proposition 1 stated in Section 3.4. Throughout, we compare two architectures under a common system boundary and a common primary energy input from waste.

### A.1 Setup and accounting conventions

Let the primary energy input rate from waste be  $\dot{E}_{in} = \dot{m}_w LHV$ . Let  $\eta_c$  denote effective conversion/utilization within the WtE boundary (combustion/boiler availability), so the primary exergy/available energy entering the conversion chain is approximated as:  $Ex_{in} \equiv \eta_c \dot{E}_{in}$ . This is a standard screening approximation for comparative statics; the proof below only requires that  $Ex_{in}$  is identical across configurations.

We define two configurations:

- Standalone configuration (S): WtE produces electricity  $\dot{W}_e$ . Recoverable heat is rejected (no credited useful output within the considered service set). DC cooling is provided mechanically using electricity.
- Coupled configuration (C): The same WtE produces  $\dot{W}_e$ . A portion of recoverable heat is delivered and converted into cooling. This requires additional parasitic work  $\dot{W}_{par}$  (pumps/controls/auxiliaries for thermal delivery and absorption). We credit the cooling service by its exergy content.

**Credited useful outputs.** We credit two services as useful outputs within the coupled boundary:

1. **Electricity** available for externally useful purposes (including supplying computing loads).
2. **Cooling service** delivered to the DC, credited by its exergy content.

Let  $T_0$  be ambient temperature and  $T_c$  the chilled-water (or evaporator) temperature. The exergy factor of a cooling effect is:  $\phi_c \equiv \frac{T_0}{T_c} - 1 > 0$ , so the exergy of a cooling flow  $\dot{Q}_{cool}$  is:  $Ex_{cool} \equiv \phi_c \dot{Q}_{cool}$ .

**Net useful exergy output.** A key point is that parasitic work  $\dot{W}_{par}$  is not “free”: it consumes high-grade electricity and should be treated as a reduction in net useful output within the same boundary.

Hence we define net useful exergy output as:

- Standalone:  $Ex_{out,net}^{(S)} \equiv \dot{W}_e$
- Coupled:  $Ex_{out,net}^{(C)} \equiv \dot{W}_e - \dot{W}_{par} + \phi_c \dot{Q}_{cool}$ .

This net-output definition is conservative and audit-friendly: it credits cooling only by its exergy content and explicitly debits parasitic high-grade work.

### A.2 Proposition and proof

*Proposition 1 (Sufficient condition).*

Holding the primary input  $Ex_{in}$  fixed, a sufficient condition for the coupled architecture to weakly dominate the standalone architecture in systemic exergy utilization is:

$$\phi_c \dot{Q}_{cool} \geq \dot{W}_{par}. \quad (\text{A1})$$

Proof

Given identical  $Ex_{in}$  across configurations, dominance in exergy efficiency is equivalent to dominance in net useful exergy output, because:

$$\eta_{ex,net}^{(k)} \equiv \frac{Ex_{out,net}^{(k)}}{Ex_{in}}, k \in \{S, C\}$$

Thus  $\eta_{ex,net}^{(C)} \geq \eta_{ex,net}^{(S)}$  if and only if  $Ex_{out,net}^{(C)} \geq Ex_{out,net}^{(S)}$ .

Compute the difference:

$$Ex_{out,net}^{(C)} - Ex_{out,net}^{(S)} = (\dot{W}_e - \dot{W}_{par} + \phi_c \dot{Q}_{cool}) - \dot{W}_e = \phi_c \dot{Q}_{cool} - \dot{W}_{par} \quad (A2)$$

Therefore, if  $\phi_c \dot{Q}_{cool} - \dot{W}_{par} \geq 0$ , then  $Ex_{out,net}^{(C)} \geq Ex_{out,net}^{(S)}$ , implying:  $\eta_{ex,net}^{(C)} \geq \eta_{ex,net}^{(S)}$

This proves (A1) is sufficient. ■

### A.3 Interpreting the condition as a grade-matching criterion

Condition (A1) can be read as a grade-matching inequality: the quality-adjusted benefit from converting low-grade heat into cooling must exceed the high-grade work required to deliver and realize that conversion.

Using the model in Section 3,  $\dot{Q}_{cool} = COP_{abs} \eta_{tr}(L) \dot{Q}_h$ , the sufficient condition becomes:

$$\phi_c COP_{abs} \eta_{tr}(L) \dot{Q}_h \geq \dot{W}_{par} \quad (A3)$$

Because  $\eta_{tr}(L)$  is decreasing in distance, (A3) immediately implies the existence of a distance-dependent break-even region for thermoeconomic dominance.

### A.4 Remarks on strength and scope (why “sufficient”)

- The condition is sufficient, not necessary: the coupled system may still be attractive under alternative objective functions (e.g., grid-capacity relief, carbon intensity reduction, or electric OpEx savings) even when (A1) fails.
- The condition relies only on (i) consistent system boundaries, (ii) a conservative exergy credit for cooling, and (iii) explicit debiting of parasitic high-grade work, precisely the elements that prevent metric-gaming critiques.

## Appendix B. Derivations for Comparative Statics and Threshold Conditions (for Section IV)

This appendix collects the formal expressions underlying Section 4's comparative statics. The main text can focus on results and decision relevance while referencing this appendix for derivations.

### B.1 Recoverable heat, delivered heat, and cooling coverage

From Section 3, with  $\dot{E}_{in} = \dot{m}_w LHV$  and net electric output  $\dot{W}_e = \eta_e \eta_c \dot{E}_{in}$ , recoverable heat is:

$$\dot{Q}_h = \alpha_h (\eta_c \dot{E}_{in} - \dot{W}_e) = \alpha_h (\eta_c - \eta_e \eta_c) \dot{E}_{in} = \alpha_h \eta_c (1 - \eta_e) \dot{E}_{in} \quad (B1)$$

Thermal delivery is reduced-form:

$$\dot{Q}_{del} = \eta_{tr}(L) \dot{Q}_h, \eta_{tr}(L) = e^{-\beta L} \quad (B2)$$

Cooling produced by absorption:

$$\dot{Q}_{cool} = COP_{abs} \dot{Q}_{del} = COP_{abs} \eta_{tr}(L) \dot{Q}_h \quad (B3)$$

Cooling requirement is parameterized as:

$$\dot{Q}_{req} = \gamma \dot{W}_{IT} \quad (B4)$$

Define coverage share:

$$f \equiv \min \left\{ 1, \frac{\dot{Q}_{cool}}{\dot{Q}_{req}} \right\} = \min \left\{ 1, \frac{COP_{abs} \eta_{tr}(L) \dot{Q}_h}{\gamma \dot{W}_{IT}} \right\} \quad (B5)$$

Equation (B5) is the workhorse for utilization, feedstock, climate, and distance sensitivities.

### B.2 Electric cooling power and electric PUE expression

Residual cooling not covered thermally is  $(1 - f) \dot{Q}_{req}$ , met mechanically with COP  $COP_m$ :

$$\dot{W}_{cool,m} = \frac{(1 - f) \dot{Q}_{req}}{COP_m} = \frac{(1 - f) \gamma \dot{W}_{IT}}{COP_m}. \quad (B6)$$

Define electric PUE (facility electricity accounting):

$$PUE_{elec} = \frac{\dot{W}_{IT} + \dot{W}_{aux} + \dot{W}_{cool,m} + \dot{W}_{par}}{\dot{W}_{IT}} = 1 + \frac{\dot{W}_{aux}}{\dot{W}_{IT}} + \frac{(1 - f) \gamma}{COP_m} + \frac{\dot{W}_{par}}{\dot{W}_{IT}} \quad (B7)$$

Standalone benchmark (no thermal coverage)

Standalone corresponds to  $f = 0$  and  $\dot{W}_{par} = 0$ , giving:

$$PUE_{elec}^{(S)} = 1 + \frac{\dot{W}_{aux}}{\dot{W}_{IT}} + \frac{\gamma}{COP_m} \quad (B8)$$

Coupled improvement in electric PUE

Subtract (B7) from (B8):

$$PUE_{elec}^{(S)} - PUE_{elec}^{(C)} = \frac{f \gamma}{COP_m} - \frac{\dot{W}_{par}}{\dot{W}_{IT}} \quad (B9)$$

Thus, coupling improves electric PUE whenever:

$$\frac{f \gamma}{COP_m} \geq \frac{\dot{W}_{par}}{\dot{W}_{IT}} \quad (B10)$$

This is an electricity-centric (grid-relief/OpEx) condition distinct from the exergy-centric Proposition in Appendix A.

### B.3 Full-coverage condition and utilization threshold

Full coverage occurs when  $\dot{Q}_{cool} \geq \dot{Q}_{req}$ , i.e.,  $f = 1$ . Using (B3)–(B4):

$$COP_{abs} \eta_{tr}(L) \dot{Q}_h \geq \gamma \dot{W}_{IT} \quad (B11)$$

This condition can be inverted to obtain an IT load ceiling that can be fully cooled thermally:

$$\dot{W}_{IT} \leq \frac{COP_{abs}\eta_{tr}(L)\dot{Q}_h}{\gamma} \quad (B12)$$

If IT utilization is represented by  $\rho \in (0,1]$  such that  $\dot{W}_{IT} = \rho \dot{W}_{IT,max}$ , then (B12) gives:

$$\rho \leq \frac{COP_{abs}\eta_{tr}(L)\dot{Q}_h}{\gamma \dot{W}_{IT,max}} \quad (B13)$$

This expression directly supports the utilization-based comparative static (Fig 1): higher  $\rho$  praises cooling demand linearly while coverage depends on available delivered heat.

#### B.4 Exergy efficiency and its parametric dependence

Define cooling exergy factor:

$$\phi_c = \frac{T_0}{T_c} - 1 \quad (B14)$$

Cooling exergy:

$$Ex_{cool} = \phi_c \dot{Q}_{cool} \quad (B15)$$

Systemic exergy efficiency (gross, before debiting parasitics) as in main text:

$$\eta_{ex} = \frac{\dot{W}_e + \phi_c \dot{Q}_{cool}}{\eta_c \dot{E}_{in}} \quad (B16)$$

Substitute (B3) and (B1):

$$\eta_{ex} = \frac{\dot{W}_e + \phi_c COP_{abs}\eta_{tr}(L)\dot{Q}_h}{\eta_c \dot{E}_{in}} = \frac{\eta_e \eta_c \dot{E}_{in} + \phi_c COP_{abs}\eta_{tr}(L)\alpha_h \eta_c (1 - \eta_e) \dot{E}_{in}}{\eta_c \dot{E}_{in}} \quad (B17)$$

Canceling  $\eta_c \dot{E}_{in}$  yields a compact form:

$$\eta_{ex} = \eta_e + \phi_c COP_{abs} \eta_{tr}(L) \alpha_h (1 - \eta_e) \quad (B18)$$

Equation (B18) makes the comparative statics transparent:

- $\frac{\partial \eta_{ex}}{\partial COP_{abs}} > 0$ ,
- $\frac{\partial \eta_{ex}}{\partial \eta_{tr}} > 0$ ,
- $\frac{\partial \eta_{ex}}{\partial \phi_c} > 0$ ,
- $\frac{\partial \eta_{ex}}{\partial \alpha_h} > 0$ .

*Net exergy efficiency (debiting parasitics)*

If one prefers exergy efficiency net of parasitic work (consistent with Appendix A):

$$\eta_{ex,net} = \frac{\dot{W}_e - \dot{W}_{par} + \phi_c \dot{Q}_{cool}}{\eta_c \dot{E}_{in}} \quad (B19)$$

#### B.5 Distance thresholds (coverage and thermoeconomic break-even)

With  $\eta_{tr}(L) = e^{-\beta L}$ , two thresholds are particularly decision-relevant.

##### B.5.1 Coverage break-even distance $L_{max}$

From full coverage condition (B11):

$$COP_{abs} e^{-\beta L} \dot{Q}_h \geq \gamma \dot{W}_{IT}$$

Rearranging:

$$e^{-\beta L} \geq \frac{\gamma \dot{W}_{IT}}{COP_{abs} \dot{Q}_h} \Rightarrow L \leq \frac{1}{\beta} \ln \left( \frac{COP_{abs} \dot{Q}_h}{\gamma \dot{W}_{IT}} \right) \quad (B20)$$

Define:

$$L_{max} \equiv \frac{1}{\beta} \ln \left( \frac{COP_{abs} \dot{Q}_h}{\gamma \dot{W}_{IT}} \right) \quad (B21)$$

When  $L > L_{max}$ , thermal cooling becomes partial ( $f < 1$ ).

### B.5.2 Thermoconomic break-even distance $L_{max}$

Using the sufficient condition in Appendix A (A3):

$$\phi_c COP_{abs} e^{-\beta L} \dot{Q}_h \geq \dot{W}_{par}$$

Rearranging gives:

$$L \leq \frac{1}{\beta} \ln \left( \frac{\phi_c COP_{abs} \dot{Q}_h}{\dot{W}_{par}} \right) \quad (B22)$$

Define:

$$L_{max} \equiv \frac{1}{\beta} \ln \left( \frac{\phi_c COP_{abs} \dot{Q}_h}{\dot{W}_{par}} \right) \quad (B23)$$

This threshold is typically (weakly) more stringent than  $L_{max}$  when parasitic work is non-negligible.

### B.6 Feedstock sensitivity: $LHV$ and waste flow $\dot{m}_w$

From (B1),  $\dot{Q}_h \propto \dot{E}_{in} = \dot{m}_w LHV$ . Specifically:

$$\dot{Q}_h = \alpha_h \eta_c (1 - \eta_e) \dot{m}_w LHV \quad (B24)$$

Substituting (B24) into (B5), coverage share becomes:

$$f = \min \left\{ 1, \frac{COP_{abs} \eta_{tr}(L) \alpha_h \eta_c (1 - \eta_e) \dot{m}_w LHV}{\gamma \dot{W}_{IT}} \right\} \quad (B25)$$

Thus, in the interior region where  $f < 1$ ,

$$f \propto \dot{m}_w \cdot LHV \quad (B26)$$

This yields a clean interpretation for Section 4: higher waste throughput or higher calorific value increases delivered heat and therefore increases cooling coverage, improving  $PUE_{elec}$  via (B7) and increasing  $\eta_{ex}$  via (B18).

### B.7 Climate-band sensitivity: reduced-form parameterization

Climate affects comparative statics primarily through:

1. The cooling requirement coefficient  $\gamma$  (how much cooling is needed per unit IT load).
2. Mechanical chiller performance  $COP_m$ .

A reduced-form parameterization suitable for screening-level analysis is:

$$\gamma = \gamma(T_{wb}), COP_m = COP_m(T_{wb}), \quad (B27)$$

where  $T_{wb}$  denotes wet-bulb temperature (or a climatic proxy). For example, one may use linear or piecewise-linear approximations around representative bands:

$$\gamma(T_{wb}) \approx \gamma_0 + \gamma_1(T_{wb} - \bar{T}_{wb}), COP_m(T_{wb}) \approx c_0 - c_1(T_{wb} - \bar{T}_{wb}), \quad (B28)$$

with  $\gamma_1 > 0$  and  $c_1 > 0$  capturing the intuitive facts that hotter/more humid conditions increase cooling demand and reduce mechanical efficiency.

Substituting (B27) into (B7) and (B5) shows climate affects both the numerator (cooling electricity) and the coverage ratio  $f$  through  $\gamma$ . This supports a climate-band comparative static without requiring equipment-level psychrometric modeling.

### B.8 Parasitic-work specification and robustness

In Section 3 we used a reduced-form representation:

$$\dot{W}_{par} = \kappa_0 + \kappa_1 \dot{W}_{IT} + \kappa_2 L \quad (B29)$$

This allows transparent robustness checks:

- $\kappa_1$  governs scale effects (whether parasitics scale sublinearly or linearly with IT load),
- $\kappa_2$  captures distance-dependent pumping/controls burdens.

Combining (B29) with (B23) yields an implicit distance feasibility condition that is more realistic when parasitics increase with  $L$ .

### B.9 Summary of the decision-relevant inequalities (for quick reference)

For convenience, we collect the core inequalities used for screening:

(i) Full thermal coverage (no mechanical cooling):

$$COP_{abs}\eta_{tr}(L)\dot{Q}_h \geq \gamma \dot{W}_{IT} \quad (B30)$$

(ii) Electric PUE improvement (grid electricity intensity improves):

$$\frac{f\gamma}{COP_m} \geq \frac{\dot{W}_{par}}{\dot{W}_{IT}} \quad (B31)$$

(iii) Thermo-economic superiority (exergy-based sufficient condition):

$$\phi_c \dot{Q}_{cool} \geq \dot{W}_{par} \Leftrightarrow \phi_c COP_{abs}\eta_{tr}(L)\dot{Q}_h \geq \dot{W}_{par} \quad (B32)$$

These conditions separate three distinct notions of “benefit”: operational feasibility (coverage), electricity-system relief (electric PUE), and quality-adjusted utilization (exergy).

Overall, the paper’s contribution is a compact, defensible framework for evaluating WtE–AIDC coupling as an infrastructure decision under AI-driven grid stress. The core takeaway is not that “WtE is the answer,” but that cooling is a scarce energy service and grade matching can restructure urban infrastructure so that waste treatment becomes a cooling-enabling asset for compute deployment. By providing transparent accounting boundaries, sensitivity-aware break-even logic, and finance-readable cost and ESG interfaces, the framework supports the kind of decision-ready analysis needed for practical planning of AI data-center corridors.

## Appendix C. Parameterization and Scenario Table

### C.1 Purpose and reproducibility boundary

This appendix documents the parameterization and scenario construction used to generate the quantitative results (Figs. 3–6) and sensitivity bands. The modeling objective is screening-level corridor feasibility for a coupled WtE–AIDC topology under spatial decay and parasitic constraints, not detailed equipment design. Accordingly, parameters are anchored to published ranges for (i) MSW energy content and representative WtE steam/hot-water conditions, (ii) absorption chilling performance as a function of driving temperature, and (iii) district-energy transport losses, pumping electricity, and network costs.

Reproducibility is ensured by: (a) explicit definitions of each parameter and its unit; (b) a scenario table with conservative/base/aggressive values; and (c) a transparent mapping from published physical measures (e.g., pipe heat loss in W/m) into the reduced-form corridor parameters used in the paper (e.g., thermal decay rate  $\beta$  in 1/km).

### C.2 Parameter classes and definitions

#### C.2.1 Waste-to-Energy (WtE) thermal supply block

We characterize the WtE plant by the recoverable thermal stream available for coupling. For screening, we parameterize thermal availability by:

- MSW lower heating value  $LHV_{MSW}$ (MJ/kg, as received).
- Throughput  $\dot{m}_{MSW}$ (t/day).
- Net thermal fraction available for export  $\eta_{th,export}$ (dimensionless), which implicitly captures boiler efficiency, internal heat use, and the fraction not committed to electricity generation or internal processes.

We distinguish two practical export forms:

1. Steam export (typical modern WtE steam conditions are often reported around 40 bar and 400°C as a reference design point; higher parameters exist but require corrosion control).
2. Hot-water export suitable for district energy (e.g., 70–120°C supply bands depending on network generation and application).

These temperature levels matter because absorption COP depends on the driving heat temperature band.

#### C.2.2 Thermal-to-cooling conversion (absorption) block

Absorption performance is parameterized by the thermal COP:

$$COP_{abs} = \frac{Q_{cool}}{Q_{drive}}.$$

We use published ranges for LiBr–H<sub>2</sub>O absorption chillers:

- Single-effect: typically requires ~80–100°C driving heat and commonly operates around COP  $\approx 0.7$ –0.8.
- Double-effect / direct-fired equivalents: commonly reported COP ranges cluster around ~0.9–1.2, with higher values under favorable configurations and conditions.

In all scenarios,  $COP_{abs}$  is evaluated consistently with the assumed driving temperature band  $T_{drive}$  and the cooling-water temperature (or condenser/absorber sink temperature), which is climate-dependent.

#### C.2.3 Corridor delivery: thermal decay and pumping parasitics

The corridor is represented as a single trunk delivery path of length  $L$ (km), capturing two first-order feasibility constraints:

(i) Thermal delivery decay. We model delivered driving heat as:

$$Q_{\text{drive,del}}(L) = Q_{\text{drive,0}} \exp(-\beta L),$$

where  $\beta(1/\text{km})$  is a reduced-form parameter representing aggregate transport losses (insulation loss + return effects + unavoidable dispersion). To anchor  $\beta$  to measurable engineering quantities, we map from pipe linear heat loss  $q_\ell(\text{W/m})$  via:

$$\beta \approx \frac{(q_\ell \cdot 1000)}{Q_{\text{trunk}}} \text{ for small losses,}$$

where  $Q_{\text{trunk}}$  is the representative thermal flow in the trunk (W). Published pipe guides and examples commonly express heat loss in W/m and show values in the order of 10–40 W/m depending on temperature difference and insulation standard; the implied  $\beta$  therefore depends on trunk loading (higher trunk flow yields smaller fractional loss per km). We explicitly report the implied  $\beta$  bands in Table C1.

(ii) Pumping electricity. We parameterize pumping electricity as a specific electric intensity:

$$e_{\text{pump}} = \frac{W_{\text{pump}}}{Q_{\text{del}}} (\text{kWh}_e/\text{MWh}_{\text{th}}),$$

and/or as a fraction of delivered thermal power under the assumed conversion chain. Recent district-heating modeling studies report pumping electricity on the order of a few  $\text{kWh}_e$  per  $\text{MWh}_{\text{th}}$  (with higher values possible under low-temperature/4GDH configurations or unfavorable hydraulics). We adopt scenario bands centered on this literature.

#### C.2.4 Data-center demand and baseline cooling electricity

We express the AI data center by:

- IT power capacity  $P_{\text{IT}}(\text{MW})$ .
- Utilization  $u \in [0,1]$  such that average IT load is  $uP_{\text{IT}}$ .
- Baseline facility performance via  $PUE_{\text{base}}$  (dimensionless), used only to represent the baseline “electric-to-cooling” boundary condition.

To avoid confusion with ISO/IEC PUE comparability, the paper’s service-adjusted metric (if used) should be treated as a separate accounting object (see Section 3); in this appendix we only parameterize baseline PUE as a boundary condition that governs baseline non-IT electricity.

#### C.3 Scenario construction (Conservative / Baseline / Aggressive)

We define three scenario packages to transparently separate:

- Engineering realism and uncertainty (losses, COP, pumping),
- Economic context (electricity price, discount rate, capital intensity),
- Climate boundary conditions (sink temperature / wet-bulb proxies).

Conservative assumptions are intentionally unfavorable to coupling (higher decay, lower COP, higher pumping, lower electricity price). Aggressive assumptions represent favorable but still literature-consistent conditions (lower decay, higher COP, lower pumping, higher electricity price). Baseline sits at literature midpoints.

Table C1. Core parameters and scenario values (used for Figs. 3–6 and sensitivity bands)

Notation: “C/B/A” = Conservative / Baseline / Aggressive. Where a parameter is derived (not directly assumed), we report the derivation mapping.

Parameter	Symbol	Unit	Cons	Baseline	Aggres	Definition / how used	Anchoring notes (source)
MSW lower heating value (as received)	$LHV_{MSW}$	MJ/kg	8	10	12	Feedstock energy content driving recoverable heat	Reported MSW LHV commonly ~8–12 MJ/kg; average ~10 MJ/kg appears frequently in the MSW/WtE literature (Source C3, C4).
WtE throughput (representative plant)	$\dot{m}_{MSW}$	t/day	500	1500	3000	Scales available chemical energy and thermal export	Large facilities commonly exceed hundreds to thousands t/day; used only as scaling input for $Q_{drive,0}$ (Source C7 for regulatory threshold context; plant scale examples widely reported).
Exportable thermal fraction (net)	$\eta_{th,export}$	–	0.30	0.45	0.60	Converts MSW chemical energy into exportable driving heat stream	Screening parameter capturing boiler efficiency, internal loads, and export share; reported here as scenario lever; users can replace with plant-specific heat balance.
Reference steam conditions (for context)	–	bar, °C	40 bar, 400°C	40 bar, 400°C	40 bar, 400°C	Context for “modern WtE” steam availability; not a decision variable	Typical WtE steam conditions often cited around 40 bar, 400°C; higher parameters exist with corrosion control (Source C5).
Driving heat temperature band (hot-water equivalent)	$T_{drive}$	°C	80	90	110	Determines feasible absorption configuration and COP band	Single-effect LiBr commonly requires ~80–100°C driving heat (Source C1).
Absorption COP (single-effect band)	$COP_{abs}$	–	0.65	0.75	0.85	Converts delivered driving heat into delivered cooling	Published single-effect COP typically ~0.6–0.8; values ~0.7–0.8 commonly reported (Source C1, C2).
Climate sink proxy (cooling-water temperature)	$T_{cw}$	°C	30	27	24	Affects achievable COP and auxiliary power; implemented as scenario boundary	Represents hot/humid vs moderate vs cool/dry bands; can be tied to wet-bulb + approach if desired.
Pipe linear heat loss (modern insulated)	$q_e$	W/m	40	25	10	Intermediate anchor used to derive $\beta$ band	Pipe guides and examples report heat loss in W/m; 10–40 W/m is representative across $\Delta T$ and insulation classes (Source C6).
Representative trunk thermal flow (for mapping)	$Q_{trunk}$	$MW_{th}$	2	5	10	Used to translate $q_e$ into $\beta$ via $\beta \approx (q_e \cdot 1000) / Q_{trunk}$	Makes explicit that fractional loss depends on load level; can be replaced with plant/network design flow.
Thermal decay rate (implied)	$\beta$	1/km	0.020	0.005	0.001	Used in $Q_{drive,del} = Q_{drive,0} \exp(-\beta L)$	These values correspond to the $q_e$ and $Q_{trunk}$ anchors above; reported as the reduced-form corridor decay parameter.
Pumping electricity intensity	$e_{pump}$	kWh <sub>e</sub> / MWh <sub>th</sub>	10	6	2	Converts delivered thermal flow into required pumping electricity	Recent district-heating modeling reports values around several kWh <sub>e</sub> / MWh <sub>th</sub> (e.g., ~6 in 4GDH cases) (Source C8).
Pump+auxiliary fraction at absorber plant	$\alpha_{aux}$	% of $Q_{cool}$ (as electric equiv.)	6%	4%	2%	Captures absorber auxiliaries, cooling-tower fan/pump equivalents, and controls	Used to prevent “free cooling” artifacts; conservative case penalizes auxiliaries.
Baseline PUE (electric-only boundary)	$PUE_{base}$	–	1.50	1.35	1.20	Baseline facility electricity burden (IT + support)	Screening boundary condition; not claimed as ISO-comparable after service substitution.
Electricity price	$p_e$	\$/kWh	0.06	0.12	0.18	Used in LCOE and break-even economics	Represents regional variation; conservative uses low price (less benefit from avoided electricity).
Discount rate (real)	$r$	%	10%	7%	5%	Used in annualization of CAPEX in LCOE	Screening financial assumption; replaceable with project WACC.
Pipe network CAPEX (installed, supply-return, inclusive)	$c_{pipe}$	\$/m	1200	750	500	Used to translate distance into CAPEX penalty	District heating distribution network construction cost around \$750/m for typical network diameters is reported in techno-economic modeling literature; we adopt scenario bands around this anchor (Source C9).

Table C2. Scenario packages used for primary figures

Package	Engineering (loss/COP/pumping)	Climate sink	Economic context	Intended interpretation
Conservative	High $\beta$ , low $COP_{abs}$ , high $e_{pump}$ , higher $\alpha_{aux}$	Hotter sink (higher $T_{cw}$ )	Lower $p_e$ , higher $r$ , higher $c_{pipe}$	Lower-bound feasibility; “corridor shrinks quickly” under unfavorable but plausible conditions
Baseline	Midpoint $\beta$ , midpoint $COP_{abs}$ , midpoint $e_{pump}$	Moderate sink	Midpoint prices/discount/cost	Representative screening case
Aggressive	Low $\beta$ , higher $COP_{abs}$ , low $e_{pump}$ , low $\alpha_{aux}$	Cooler sink	Higher $p_e$ , lower $r$ , lower $c_{pipe}$	Upper-bound feasibility envelope; still literature-consistent

#### C.4 Minimal “how to reproduce” checklist (for the editor)

To reproduce Figs. 3–6:

1. Select a scenario package (Table C2) and associated parameters (Table C1).
2. Compute available exportable driving heat  $Q_{drive,0}$  from  $LHV_{MSW}$ ,  $\dot{m}_{MSW}$ , and  $\eta_{th,export}$  (or substitute a plant-specific heat balance).
3. Apply corridor decay to obtain  $Q_{drive,del}(L) = Q_{drive,0} \exp(-\beta L)$ .
4. Convert to delivered cooling  $Q_{cool}(L) = COP_{abs} \cdot Q_{drive,del}(L)$ , and subtract electric-equivalent auxiliaries using  $\alpha_{aux}$ .

5. Compute pumping electricity using  $e_{\text{pump}}$  and delivered thermal flow (and include it in total electricity burden).
6. Compare against the baseline electric-cooling boundary derived from  $PUE_{\text{base}}$ ,  $P_{\text{IT}}$ , and utilization  $u$ , producing coverage/break-even and any accounting metrics (including LCOC in Section 5, if applied).